



HAL
open science

Effect of plastic straining on the remanent magnetization of ferritic-pearlitic steel: Experimental and modeling aspects

Z. Maazaz, Olivier Hubert, E. Amira Fnaiech, L. Kassir

► **To cite this version:**

Z. Maazaz, Olivier Hubert, E. Amira Fnaiech, L. Kassir. Effect of plastic straining on the remanent magnetization of ferritic-pearlitic steel: Experimental and modeling aspects. *AIP Advances*, 2021, 11 (2), pp.025015. 10.1063/9.0000237 . hal-03135916

HAL Id: hal-03135916

<https://hal.science/hal-03135916>

Submitted on 9 Feb 2021

HAL is a multi-disciplinary open access archive for the deposit and dissemination of scientific research documents, whether they are published or not. The documents may come from teaching and research institutions in France or abroad, or from public or private research centers.

L'archive ouverte pluridisciplinaire **HAL**, est destinée au dépôt et à la diffusion de documents scientifiques de niveau recherche, publiés ou non, émanant des établissements d'enseignement et de recherche français ou étrangers, des laboratoires publics ou privés.

Effect of plastic straining on the remanent magnetization of ferritic-pearlitic steel: experimental and modeling aspects

Z. Maazaz,^{1,2, a)} O. Hubert,^{1, b)} E. Amira Fnaiech,² and L. Kassir^{2, c)}

¹⁾*Université Paris-Saclay, ENS Paris-Saclay, CNRS, LMT -
Laboratoire de Mécanique et Technologie, 91190 Gif-sur-Yvette,
France.*

²⁾*Skipper NDT, 75015 Paris, France.*

(Dated: 9 February 2021)

The remanent magnetization of a carbon steel which has been plastically deformed by uniaxial tensile test at different strain levels is measured along the tensile direction during unloading and at the unloaded state. It is shown that plastic strain considerably reduces the remanent magnetization but that remanence is recovered under applied stress, leading to the conclusion that behavior of the deformed material seems to be able to be obtained by a simple translation in the stress space of the behavior at the undeformed state. This result is in accordance with the results of a modeling approach considering the deformed material as a two phase material submitted to a strong internal stress level.

^{a)}Electronic mail: zakariae.maazaz@ens-paris-saclay.fr

^{b)}Electronic mail: olivier.hubert@ens-paris-saclay.fr

^{c)}Electronic mail: l.kassir@skipperndt.com

I. INTRODUCTION

Steel is widely used in infrastructures such as oil/gas pipelines and hanging bridges. The modification of the state of this material affects hugely its magnetic behavior¹. Non-destructive testing of materials usually involves the measurement of a physical quantity in relation with the modification of a physical property of the material. Some recent nondestructive testing methods have been developed to detect very small variations in the magnetic field surrounding a massive ferromagnetic structure, such as a tank or pipe². In particular, the detection of sinking in buried pipelines becomes possible³. The sinking is characterized by local plastic deformation and the creation of long range residual stresses. These two elements are known to have a considerable influence on the magnetic behavior⁴⁵⁶⁷. One of the keys to detect a sinking is the substantial modification of the remanent magnetization of the material. However, reverse identification of defects requires models allowing the association of the remanent magnetization to a given mechanical state. This work gives first insight of what can be done in this direction. The first part of the paper presents an experimental study where the variation of magnetic behavior (especially remanent magnetization) according to stress and strain is illustrated. The modeling principles are then presented in the second part and applied to analyze the experimental results. Discussion and conclusion finalize this work.

II. MATERIAL, EXPERIMENTAL PROTOCOL AND RESULTS

A. Material and experimental protocol

A pipeline steel (wt.%C=0.19; wt.%Mn=0.85, wt.%Si=0.2) has been used in the study. Its microstructure presented in figure 1 consists of about 40%vol. of pearlite islands aligned along the pipe direction in a ferritic matrix. The combination of the two phases leads to a soft ferromagnetic behavior. The microstructure exhibits a preferential orientation in accordance with a forming process made of successive rollings and annealings. The specimens for mechanical and magnetic testings are taken from a 150 mm diameter tube, along its axial direction. They are 180 mm long, 12 mm wide, and 4 mm thick strips. The experimental magnetic device enables magnetic measurements, under low-frequency (0.2Hz) triangular magnetic field conditions. The magnetic set-up is composed of a primary coil to magnetize the sample, a pick-up coil (B-coil) to measure the electromotive force, two ferrite yokes designed to close the magnetic circuit and reduce the

macroscopic demagnetizing field (please refer to⁸ for more details about set-up and procedure). Measurements have been first performed on unstrained samples providing the reference magnetic behavior. Samples are next positioned between the jaws of a MTS uniaxial electrohydraulic (displacement controlled) machine. Measurements have been performed on samples submitted to an increasing plastic deformation level during mechanical unloading, at the unloaded state and during mechanical reloading. Only results at the unloaded state and during unloading are reported. A concomitant uniaxial stress-strain $\sigma(\epsilon)$ behavior is obtained from force and displacement measurements. It has been on the other hand verified that each unloading has a negligible cumulative effect on the global evolution of the stress-strain and magnetization behavior. The procedure has been applied to another sample to verify the reproducibility of results.

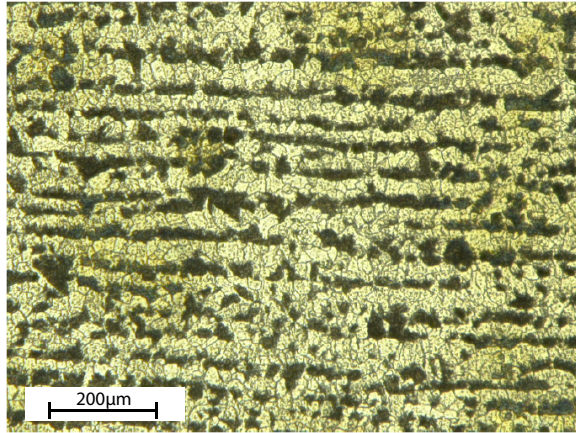


FIG. 1: Microstructure of the pipeline steel.

B. Experimental results

The uniaxial stress - longitudinal plastic strain behavior $\sigma(\epsilon_p)$ of the material is reported in red curve in figure 3b. Table I gathers the main macroscopic mechanical parameters extracted from the test. The mechanical strengthening of a material is usually related to different strengthening mechanisms, leading to the following partition:

$$\sigma = \sigma_0 + R + X' \quad (1)$$

with σ_0 the yield stress, R the isotropic hardening of the material, and X' the kinematic hardening. These parameters can be determined thanks to a set of mechanical loading and unloading: the specimen is loaded up to $p\%$ deformation, then it is unloaded until the appearance of non-linearity

TABLE I: Main mechanical parameters of pipeline steel

Young's module E (GPa)	200
Yield stress σ_0 (MPa)	340
Ultimate stress σ_u (MPa)	612

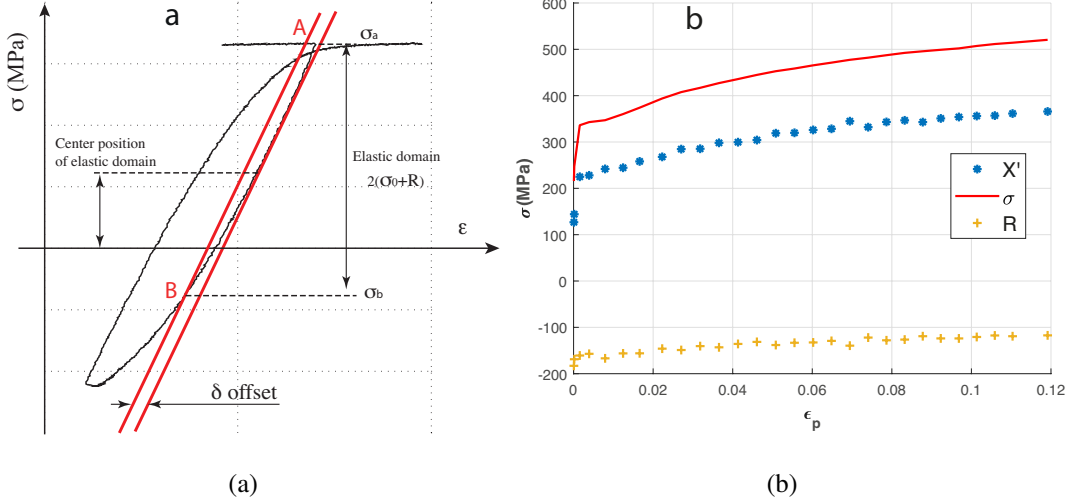


FIG. 2: (a) Experimental loading / unloading cycles for the identification of hardening parameters using the Cottrell's method⁸. (b) Estimated isotropic (R) and kinematic (X') hardenings during plastic straining.

in the compression curve. We repeat the same procedure until a strain of 15%. This precise evaluation of stress-strain loops as illustrated in figure 2(a) requires the use of an accurate extensometer (axial MTS 632.53F-11) and a dedicated sample.

The stress partition is performed using the Cottrell method⁹ involving the choice of appropriate offset parameter δ as illustrated in figure 2(a): at point A, the sample underwent a given plastic strain level. the specimen is unloaded until point B is reached corresponding to the yield stress in compression. The asymmetry between σ_a and σ_b is known as the Baushinger effect. The kinematic hardening X' is then calculated using the following equation :

$$X' = \sigma - \frac{\sigma_a - \sigma_b}{2} \quad (2)$$

We first estimate the maximal stress value σ_a and the minimal σ_b for each strain level $p\%$. To determine the minimal value σ_b , we considered a straining offset $\delta = 0.001\%$ (Figure 2(a)). Figure

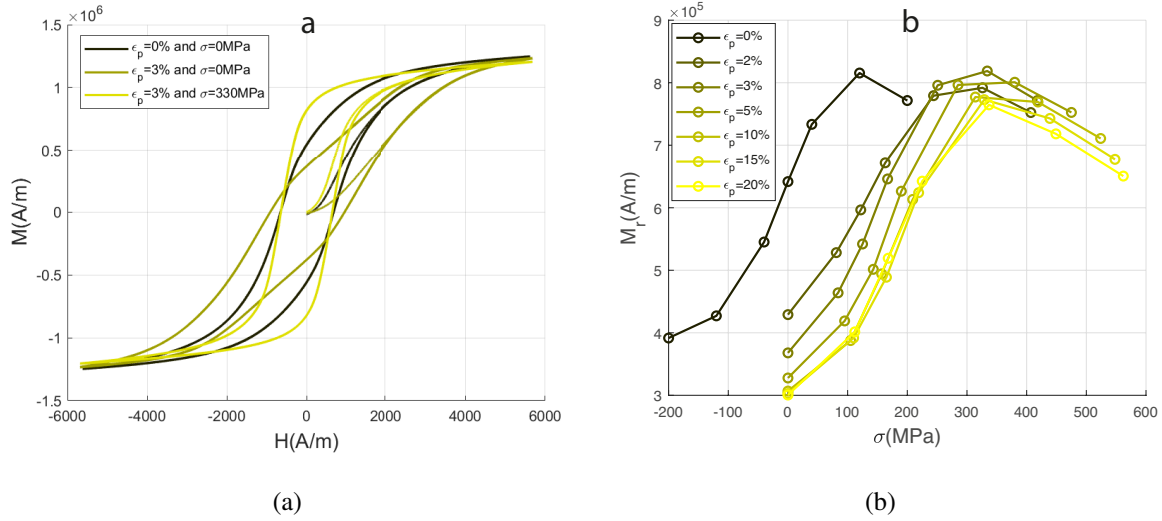


FIG. 3: (a) Hysteresis loops of dual-phase steel $f=0.2$ Hz. (b) Remanent magnetization variation according to mechanical stress $H_{max} = 5600A/m$.

2(b) shows the estimated values of X' and R as function of the plastic strain level. Figure 3(a) shows now the typical magnetic hysteresis loops obtained for the un-deformed, plastic strained samples at unloaded state and plastic strained samples under remaining loading (for a maximum magnetic field level of about 5600 A/m). As already mentioned by many authors in the literature, plastic straining leads to a strong degradation of the magnetic behavior at the unloaded state: increase of coercive field, decrease of global magnetic permeability and remanent magnetization. The magnetic behavior of the same material subjected to a superimposed high level applied stress (measurement carried out before unloading) is completely different, exhibiting material properties somehow close to or better than the reference behavior. Figure 3(b) illustrates especially the associated remanent magnetization variation as function of the applied stress and for different plastic strain levels. It is first observed that the remanent magnetization of reference material increases according to stress until stress reaches a threshold (remaining below the yield stress) where the remanent magnetization begins to decrease. These conclusions are in accordance with results reported in ⁷.

It can be observed secondly that plastic strain at the unloaded state ($\sigma=0$ MPa) leads to a strong non-linear decrease of the remanent magnetization. The variation is very strong at the first stage of plastic deformation. The evolution is slower after 2%. If we consider now the remanent magnetization under mechanical loading at a given plastic strain level (curves reported in figure

3(b)), it can be noticed that the behavior at a given plastic strain level seems to be reachable by a simple translation in the stress space: all curves seem parallel.

III. MODELING OF THE EFFECT OF PLASTICITY ON MAGNETIC BEHAVIOR

A. Modeling principle

We try in this part to give an interpretation of results obtained in the previous section. We thus based our approach on the theoretical development presented by Hubert and Lazreg⁸. We considered that the magnetic behavior of the material in the plastic state is governed by its internal stress state. In this approach, we consider a representative volume element (RVE) composed of two phases: a soft phase of volume fraction f_m and a hard phase of fraction f_d . We associate with the RVE an elastoplastic mechanical state defined by a stress tensor $\boldsymbol{\sigma}$, by an elastic strain tensor $\boldsymbol{\epsilon}_e$ and a plastic strain tensor $\boldsymbol{\epsilon}_p$.

The internal stress tensors in the soft and hard phase are given by⁸ :

$$\boldsymbol{\sigma}_m = \boldsymbol{\sigma} - \mathbf{X} \quad \text{and} \quad \boldsymbol{\sigma}_d = \boldsymbol{\sigma} + \frac{f_m}{f_d} \mathbf{X} \quad (3)$$

where \mathbf{X} is the kinematic hardening tensor, function of the plastic strain level: $\mathbf{X}(\boldsymbol{\epsilon}_p)$.

we note \mathbf{S} the stress deviator tensor defined as :

$$\mathbf{S} = \boldsymbol{\sigma} - \frac{1}{3} \text{tr}(\boldsymbol{\sigma}) \mathbf{I} \quad (4)$$

According to the early work of Hubert and Daniel¹⁰, the multi-axial magneto-mechanical equivalent stress in each phase of the material is defined by:

$$\sigma_i^{eq} = \frac{3}{2} \vec{n}^t s_i \vec{n} \quad (5)$$

where s_i is the stress deviator tensor in each phase i . By neglecting the magnetostriction effects, tensors s_i can be expressed as⁸ :

$$s_m \approx \mathbf{S} - \mathbf{X} \quad \text{and} \quad s_d \approx \mathbf{S} + \frac{f_m}{f_d} \mathbf{X} \quad (6)$$

The equivalent stress in each phase then becomes:

$$\sigma_m^{eq} = \frac{3}{2} \vec{n}^t (\mathbf{S} - \mathbf{X}) \vec{n} \quad \text{and} \quad \sigma_d^{eq} = \frac{3}{2} \vec{n}^t (\mathbf{S} + \frac{f_m}{f_d} \mathbf{X}) \vec{n} \quad (7)$$

where it is recalled that \mathbf{X} is a function of the plastic strain level and \vec{n} indicates the direction of applied magnetic field.

The magnetic behavior of a plastic strained material is finally the composition of the behavior of the two phases submitted to their own residual stress tensor :

$$\vec{M}(\vec{H}, \boldsymbol{\sigma}, \epsilon_p) = f_d \vec{M}_d(\vec{H}, \boldsymbol{\sigma}_d^{eq}(\epsilon_p), \mathbf{0}) + f_m \vec{M}_m(H, \boldsymbol{\sigma}_m^{eq}(\epsilon_p), \mathbf{0}) \quad (8)$$

We suppose next for simplicity reasons that the reference magnetic behavior of the hard and soft phases is the same, and that a constant factor k does exist, intermediate between -1 and f_m/f_d so that the following equivalent stress applies for the whole material:

$$\boldsymbol{\sigma}^{eq} = \frac{3}{2} t \vec{n} (\mathbf{S} - k \mathbf{X}) \vec{n} \quad (9)$$

leading to the following simple relationship:

$$\vec{M}(\vec{H}, \boldsymbol{\sigma}, \epsilon_p) \approx \vec{M}(\vec{H}, \boldsymbol{\sigma}^{eq}(\epsilon_p), \mathbf{0}) \quad (10)$$

This approach then makes it possible to find the values of the remanent magnetization in the plastic domain from the values of the remanent magnetization in the elastic domain (as theoretically for all magnetic properties), joining the the experimental results reported in figure 3(b) for uniaxial stress condition. Since the kinematic hardening has been identified in this experiment, an experimental evaluation of parameter k is possible.

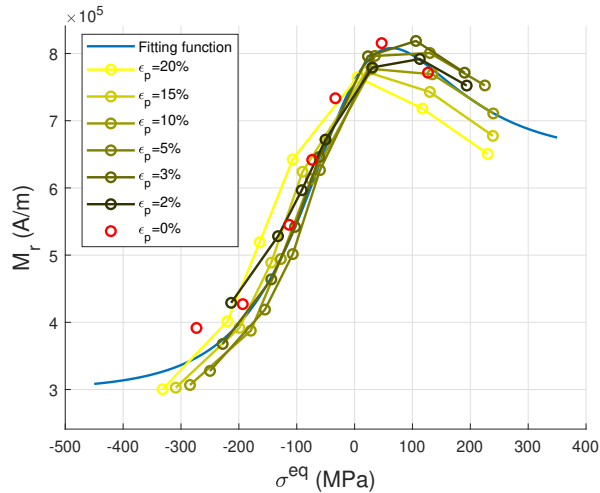


FIG. 4: Application of the equivalent stress to remanent magnetization.

TABLE II: Optimized kinematic hardening model parameters

C_{x1}	C_{x2}	γ_{s2}	C_{x3}	γ_{s3}
546 MPa	2500 MPa	30	506250 MPa	2250

B. Results and discussion

We go back to the uniaxial tensile stress condition encountered during experiments. In this situation, the equivalent stress becomes simply (since $X' = 3/2X$ where X is the uniaxial component of the kinematic stress tensor):

$$\sigma^{eq} \approx \sigma - kX' \quad (11)$$

$X'(\varepsilon_p)$ has on the other hand been modeled using a mix between a linear Prager model¹¹ and two non-linear Armstrong-Frederick models¹¹ following:

$$X'(\varepsilon_p) = C_{x1}\varepsilon_p + \frac{C_{x2}}{\gamma_{s2}}(1 - \exp(-\gamma_{s2}\varepsilon_p)) + \frac{C_{x3}}{\gamma_{s3}}(1 - \exp(-\gamma_{s3}\varepsilon_p)) \quad (12)$$

Parameters of this kinematic hardening law evaluated after minimization of the root mean square deviation between experiment and model are gathered in table II. The final point is to properly identify k parameter: indeed the ideal k parameter would allow to define the appropriate shift in the stress space of the remanent curves to find the behavior at the plastic deformed state from the undeformed state and vice-versa. Figure 4 shows the reverse application of this rule: shifting the remanent behavior curves at plastic deformed state to their theoretical behavior at undeformed state. An optimized value $k = 0.75$ has been applied for all curves, leading to a very convincing result. Such result seems to confirm the elastic origin of the plastic strain effect on magnetic behavior. Complementary experiments show however that the magnetic field level must be strong enough to get a relevant estimation of the remanent magnetization. Otherwise, rules do not apply so well.

IV. CONCLUSION

This study shows that it is possible to define a stress state that has the same effect on remanent magnetization than a plastic strain whatever the remaining applied stress. The definition of this

stress state requires to establish the kinematic strengthening of the considered material and evaluation of a unique fitting parameter k to take account of the metallurgical heterogeneities within the material. This work makes it possible to predict the local remanent magnetization state of a sinking pipeline tube thanks to the combination of an appropriate mechanical simulation of the sinking and evaluation of plastic strain and residual stress fields. This work is in progress.

DATA AVAILABILITY

The data that support the findings of this study are available from the corresponding author upon reasonable request.

REFERENCES

REFERENCES

- ¹B. Cullity, *Introduction to magnetic materials*, edited by Addison-Wesley (1972).
- ²“international patent ca2998095a1,” .
- ³E. A. Fnaiech, S. Munsch, M. Marzin, and S. Rohart, “Large stand-off magnetometry (Ism) for buried pipeline inspection: Influence of dent depth on residual magnetic signal,” Pipeline Technology Conference, Berlin (2020).
- ⁴W. H. Bozorth, R.M., “Effect of small stresses on magnetic properties,” *Reviews of Modern Physics* , 72–80 (1945).
- ⁵J. Makkar and B. Tanner, “The effect of plastic deformation and residual stress on the permeability and magnetostriction of steels,” *Journal of Magnetism and Magnetic Materials* , 222:291 (2000).
- ⁶O. Hubert, M. Clavel, I. Guillot, and E. Hug, *Jal Phys.* **IV**, p.207 (1999).
- ⁷V. Kuleev, T. Tsar’kova, and Nichipuruk, “Effect of tensile plastic deformations on the residual magnetization and initial permeability of low-carbon steels,” *Russ J Nondestruct Test* , 261–271 (2006).
- ⁸O. Hubert and S. Lazreg, “Two phase modeling of the influence of plastic strain on the magnetic and magnetostrictive behaviors of ferromagnetic materials,” *Journal of Magnetism and Magnetic Materials* **424**, 421–442 (2017).

- ⁹A. Cottrell, “Dislocations and plastic flow in crystals,” Oxford University press, London (1953).
- ¹⁰O. Hubert and L. Daniel, “Energetical and multiscale approaches for the definition of an equivalent stress for magneto-elastic couplings,” *Journal of Magnetism and Magnetic Materials* , 1766:1781 (2011).
- ¹¹J. Lemaître and J. Chaboche, *Mécanique des matériaux solides* (1988) 2ème édition Dunod, Bordas.